Auranofin induces urothelial carcinoma cell death via reactive oxygen species production and synergy with cisplatin

SAN-YUAN CHEN[1,2], CHUN-NUN CHAO[3,4], HSIN-YI HUANG[5] and CHIUNG-YAO FANG[5]

[1]Department of Chinese Medicine, Ditmanson Medical Foundation, Chiayi Christian Hospital, Chiayi 60002; [2]Department of Sports Management, Chia Nan University of Pharmacy and Science, Tainan 71710; [3]Department of Pediatrics, Ditmanson Medical Foundation, Chiayi Christian Hospital, Chiayi 60002; [4]Department of Biotechnology, Asia University, Taichung 41354; [5]Department of Medical Research, Ditmanson Medical Foundation, Chiayi Christian Hospital, Chiayi 60002, Taiwan, R.O.C.

Received September 17, 2021; Accepted November 30, 2021

DOI: 10.3892/ol.2021.13179

Abstract. Urothelial carcinoma (UC) is one of the most common cancer types of the urinary tract. UC is associated with poor 5-year survival rate, and resistance to cisplatin-based therapy remains a challenge for invasive bladder cancer treatment. Therefore, there is an urgent need to develop new drugs for advanced UC therapy. Auranofin (AF) was developed over 30 years ago for the treatment of rheumatoid arthritis and has been reported to exert an antitumor effect by increasing the level of reactive oxygen species (ROS) in cancer cells. The aim of the present study was to examine the effects of AF on cancer cell proliferation, cell cycle and apoptosis, either alone or in combination with cisplatin. AF induced cell death in two separate cell lines, HT 1376 and BFTC 909, in a concentration- and time-dependent manner by inducing cell cycle arrest. However, the distribution of cells in different phases of the cell cycle differed between the two cell lines, with G_0/G_1 cell cycle arrest in HT 1376 cells and S phase arrest in BFTC 909 cells. In addition, AF induced apoptosis in HT 1376, as well as redox imbalance in both HT 1376 and BFTC 909 cells. Cell viability was rescued following treatment with N-acetyl-L-cysteine, a ROS scavenger. Furthermore, AF treatment synergistically increased the cytotoxicity of HT 1376 and BFTC 909 cells when combined with cisplatin treatment. These findings suggest that AF may represent a potential candidate drug against UC and increase the therapeutic effect of cisplatin.

Correspondence to: Dr Chiung-Yao Fang, Department of Medical Research, Ditmanson Medical Foundation, Chiayi Christian Hospital, 539 Chung Hsiao Road, Chiayi 60002, Taiwan, R.O.C.
E-mail: fcyo@ms72.hinet.net

Key words: auranofin, urothelial carcinoma, reactive oxygen species, synergy, cisplatin

Introduction

Urothelial carcinoma (UC) is the most common malignancy of the urinary system, with ~90% cases developing in the urinary bladder and ~10% in the renal pelvis and ureter (upper tract) (1). There were ~573,000 new cases and 213,000 deaths from bladder cancer worldwide in 2020 (2), with most cases being superficial bladder cancer at initial diagnosis, and ~70% representing non-muscle-invasive bladder cancer (NMIBC) (3). Although the survival rate in patients with NMIBC is favorable, 30% will experience disease recurrence, progressing to muscle-invasive bladder cancer (MIBC) (4,5). Although radical cystectomy combined with pelvic lymph node dissection increases the survival rate in patients with MIBC, ~50% ultimately experience disease recurrence (6,7). Cisplatin-based systemic therapy plays a key role in reducing recurrence rates in patients with MIBC after local surgery (8). Although immune checkpoint inhibitors have been developed as second-line therapy for programmed cell death protein-1-positive patients, cisplatin therapy remains the standard therapy for metastatic bladder cancer. However, due to the unfavorable toxicity of cisplatin-based therapy, and only a fraction of patients achieving a disease-free survival response and chemoresistance (9), there is an urgent need to develop new drugs for the treatment of patients with UC.

Reactive oxygen species (ROS) formation and signaling play an important role in regulating physiological responses, such as metabolism, biosynthesis and cell survival (10,11). Elevated ROS levels and an alteration of the redox balance and associated signaling pathways are common in cancer cells (12,13), which may result from their compromised ROS-scavenging ability (14). Moreover, increased ROS level render cancer cells more vulnerable to ROS induction by exhausting the antioxidant system capacity in cancer cells thereby causing cell death (15). Drugs that increase ROS levels have been analyzed for their anticancer activity in biliary (16), colon (17), prostate (18), pancreatic (19) and brain cancer (20) cells. Therefore, searching for drugs that increase ROS levels in tumor cells without causing damage to normal cells may be a promising strategy for cancer therapy (21,22).

Auranofin (AF) was developed over 30 years ago for the treatment of rheumatoid arthritis (23). Recently, it has also been described as a potential anticancer agent that increases ROS levels in hepatocellular carcinoma (24), gastric cancer (25) and colorectal cancer cells (26), suggesting that cancer cells with elevated ROS levels may be vulnerable to AF treatment. ROS-producing enzymes, such as NADPH oxidase, are upregulated in UC (27,28). Therefore, AF may be a good cytotoxic drug candidate in UC cells. In the present study, two UC cell lines, HT 1376 (bladder UC) and BFTC 909 (upper-tract UC) cells, were used to examine the cytotoxicity of AF. ROS production, cell cycle profile progression and apoptosis were analyzed following AF treatment in both cell lines. The possible synergistic effect of AF and cisplatin, the gold standard chemotherapeutic agent for advanced UC, was also assessed in AF and cisplatin-treated cells. The findings of this study may provide insight into the cytotoxicity of AF in UC cells.

Materials and methods

Cell culture. The human UC cell lines, HT 1376 (bladder) and BFTC 909 (upper tract UC), were purchased from The Bioresource Collection and Research Center (Hsinchu, Taiwan, China). HT 1376 cells were cultured in minimum essential medium containing L-glutamine, non-essential amino acids and sodium pyruvate supplemented with 10% FBS (all from Gibco; Thermo Fisher Scientific, Inc.). BFTC 909 cells were cultured in 10% Dulbecco's modified Eagle's medium with L-glutamine (all Gibco; Thermo Fisher Scientific, Inc.). The two cell lines were incubated in a humidified atmosphere containing 5% CO_2 at 37˚C.

Reagents and antibodies. AF and cisplatin were purchased from Sigma-Aldrich (Merck KGaA). Mammalian Protein Extraction Reagent buffer (Thermo Fisher Scientific, Inc.) was used for protein extraction. Protease inhibitor was purchased from MilliporeSigma. Primary antibodies against apoptosis-associated proteins, including poly (ADP-ribose) polymerase (PARP; cat. no. 9542S, 1:1,000) and caspase 3 (cat. no. 9662S, 1:1,500), caspase 8 (9746S, 1:1,000), caspase 9 (9502S, 1:1,000) were purchased from Cell Signaling Technology, Inc. Antibodies specific for cell cycle-associated proteins, p21 (2947S, 1:1,000 p21), p27 (cat. no. 2552S, 1:1,000), CDK2 (2546S, 1:1,000), cyclin E2 (cat. no. 4132S, 1:1,000), CDC25A (3652S; 1:1,000), cyclin D1 (2978S, 1:1,000) were purchased from Cell Signaling Technology, Inc. Antibodies for cell-cycle-associated proteins CDK4 (GTX102993, 1:1,000), cyclin A2 (GTX103042, 1:1,000), cyclin E1 (GTX103045, 1:1,000), were purchased from GeneTex. Horseradish peroxidase-conjugated secondary goat anti-rabbit IgG (AB_2307391, 1:3,000, polyclonal) and horse anti-mouse IgG (AB_10015289, 1:3,000, polyclonal), were purchased fromJackson ImmunoReseach, Inc. The antibody against β-actin (loading control; cat. no. sc-47778, 1:7,500) was purchased from Santa Cruz Biotechnology, Inc. N-acetyl-L-cysteine (NAC; cat. no. A7250) and H_2DCFDA (D6883) were purchased from Sigma-Aldrich (Merck KGaA).

Cell viability. Cell viability was assessed using the Cell Counting Kit-8 Proliferation Assay (CCK-8; Sigma-Aldrich; Merck KGaA). Briefly, $1x10^4$ UC cells were seeded in 96-well plates, then treated with AF and incubated for 24 or 48 h at 37˚C in a humidified incubator. Viability was determined according to the manufacturer's instructions, and absorbance values were read at 490 nm 2 h after the addition of CCK-8 reagent. Values were normalized to DMSO-treated control cells. The experiments were conducted independently at least three times.

ROS analysis. To determine ROS levels, $1x10^6$ UC cells were seeded in 6-well plates at the indicated AF concentration (3 μM for HT 1376 cells and 4 μM for BFTC 909 cells) in the presence or absence of the ROS inhibitor, 3 mM NAC. The cells were treated with 10 μM H_2DCFDA (Sigma-Aldrich; Merck KGaA) at 37˚C in the dark for 30 min, washed, then analyzed using a BD FACSDiva flow cytometer (BD Biosciences). Cells stained with 10 μM H_2DCFDA only were used as a vehicle control group. The data were analyzed using FlowJo software (version 10.6.1; FlowJo LLC). The mean fluorescent intensity was calculated.

Cell cycle analysis. To determine the cell cycle distribution following AF treatment, $1x10^6$ UC cells were seeded in 6-well plates. Serum-starved cells were treated with AF, then harvested at 24 and 48 h and fixed using 100% methanol overnight at 4˚C. The fixed cells were incubated with 0.05 mg/ml propidium iodide solution containing RNase at room temperature in the dark for 30 min. The DNA content was analyzed using a BD FACSDiva flow cytometer (BD Biosciences). The percentage of cells in each phase of the cell cycle was analyzed using Modfit LT 3.3 cell cycle analysis software (Verity Software House).

Apoptosis. An annexin V-FITC Apoptosis Detection Kit (BioVision) was used to determine apoptosis in UC cells treated with AF for 24 h. HT 1376 cells were treated with 1.5 or 3 μM AF, BFTC 909 cells were treated with 2 or 4 μM AF at 37˚C for 24 h. The cells were then harvested and subjected to Annexin V staining (5 μl Annexin V-FITC and 5 μl propidium iodide in 500 μl binding buffer) at 25˚C for 5 min in the dark. The apoptotic cells were analyzed using a BD FACSDiva flow cytometer (BD Biosciences) and analyzed using BDFACSDiva software (v6.1.3; BD Biosciences). The apoptotic ratio was calculated based on the percentage early (annexin V^+ PI^-) and late (annexin V^+ PI^+) apoptotic cells.

Protein expression analysis. The protein expression in cells was analyzed after AF treatment by western blotting. The cells were lysed in Mammalian Protein Extraction Reagent (Thermo Fisher Scientific, Inc.) containing 0.1% protease inhibitor cocktail (Cell Signaling Technology, Inc.), and the protein concentration was quantified using Bio-Rad Protein Assay reagent (Bio-Rad Laboratories, Inc.). A total of 40 μg/lane protein samples were subjected to 12% SDS-PAGE and electrotransferred to a PVDF membrane. The membrane was blocked in 5% BSA (Gibco; Thermo Fisher Scientific, Inc.) and 1X TBS with 0.1% Tween-20 (Sigma-Aldrich; Merck KGaA at 25˚C for 1 h). The membrane was incubated with a primary antibody at 4˚C for 16 h. The membrane was washed with three times for 5 min each with 0.1% TBST, then incubated with a HRP-conjugated secondary antibody

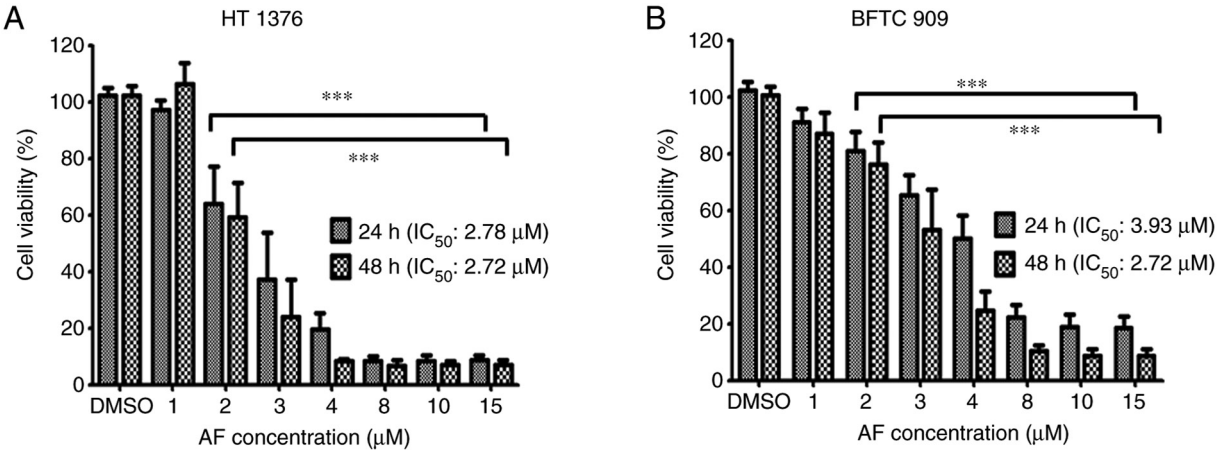

Figure 1. Effects of AF on the growth of urothelial carcinoma cells. (A) HT 1376 and (B) BFTC 909 cells were treated with the indicated concentrations of AF for 24 or 48 h. Cell viability was determined using a Cell Counting Kit-8 assay and presented as percentage cell survival. Data are representative of at least three independent experiments and shown as the mean ± SD. ***P<0.001. AF, auranofin.

(Jackson ImmunoResearch Laboratories, Inc.) for 2 h at 25˚C. The membrane was washed with three times for 5 min each with 0.1% TBST. Protein expression was detected using an enhanced chemiluminescence HRP substrate detection kit (cat. No. WBKLS0500, MilliporeSigma) and visualized using the UVP BioSpectrum 800 image system (Analytik Jena AG).

Drug combination index analysis. The Calcusyn software (Biosoft, ver. 2.0.0.0) was used to evaluate the combined effect of AF and cisplatin by calculating the combination index (CI) based on cell viability rates. The CI equation of this software is based on the multiple drug-effect equation of the Chou-Talalay method derived from enzymatic models (29). The non-constant ratio combination was used to determine the CI. Briefly, CI was determined using the equation: $(D)_1/(D_x)_1 + (D)_2/(D_x)_2 + (D)_1(D)_2/(D_x)_1(D_x)_2$. $(Dx)_1$. $(Dx)_2$ represent the doses for x% inhibition by drug 1 and drug 2, respectively. $(D)_1$ and $(D)_2$ are the combinatory doses that inhibit cell growth by x%. Fraction affect analysis was used to generate a graphic representation of the CI. CI values <0.1 indicate very strong synergism, 0.1-0.3 strong synergism, 0.3-0.7 synergism, 0.7-0.9 moderate to slight synergism, 1 nearly additive, 1.1-1.45 slight to moderate antagonism, 1.45-3.3 antagonism and >3.3 strong to very strong antagonism (30,31).

Statistical analysis. Statistical analysis was carried out using GraphPad Prism 7.0 software (GraphPad Software, Inc.). Data are presented at the mean ± SD of ≥3 experimental repeats. The data were analyzed using one-way ANOVA followed by Bonferroni correction for multiple comparisons. The *in vitro* experiments were performed in triplicate. P≤0.05 was considered to indicate a statistically significant difference.

Results

Effects of AF on the viability of UC cells. To evaluate the effect of AF on the viability of UC cells, 1, 2, 3, 4, 8, 10, and 15 μM AF were used to treat to HT 1376 and BFTC 909 cells for 24 and 48 h, and cell viability was determined using a CCK-8 assay. AF exhibited cytotoxic effects on both cell lines, with a lower IC_{50} in HT 1376 cells following 24-h treatment. The IC_{50} values for HT 1376 at 24 and 48 h were 2.78 and 2.72 μM following AF treatment, respectively (Fig. 1A). The IC_{50} for BFTC 909 was 3.93 and 2.72 μM after AF treatment at 24 and 48 h, respectively (Fig. 1B).

AF interferes with cell cycle progression in HT 1376 and BFTC 909 cells. To determine whether cell cycle progression was altered after AF treatment, HT 1376 cells were treated with 1.5 and 3 μM of AF and BFTC 909 cells were treated with 2 and 4 μM of AF, and analyzed by flow cytometry. HT 1376 cells were blocked at the G_0/G_1 phase following AF treatment, as evidenced by a concentration-dependent increase in the proportion of cells in the G_0/G_1 phase (Fig. 2A), After 1.5 and 3 μM AF treatment, G_0/G_1 phase increased from 66.06 to 71.05 at 8 h; from 65.47 to 69.74% at 12 h and from 57.00 to 65.67% at 24 h. Moreover, there was a small increase from 0.57 to 4.12% in the frequency of $subG_1$ cells following treatment with 3 μM AF, but not significant in 1.5 μM AF treated group (Fig. 2B). Cell cycle progression is regulated by the coordination of several CDKs/cyclin complexes (32,33). Having confirmed that AF caused G_0/G_1 cell cycle arrest in HT 1376 cells, the next experiments were carried out to determine the expression patterns of cell cycle-associated proteins. The CDK inhibitors, p21 and p27, inhibit the activity of cyclin D1, cyclin E1/E2 and CDK4, thereby negatively regulating cell cycle progression and causing cell arrest at the G_0/G_1 phase (34,35). In HT 1376 cells, AF treatment upregulated the expression of p21 and p27 in a concentration-dependent manner compared with the control (0 μM). In addition, decreased expression of CDK2, CDK4, cyclin D1 and cyclin E2 was observed in AF-treated HT 1376 cells (Fig. 2C). These data suggested AF treatment caused HT 1376 cells arrest at the G_0/G_1 phase.

Similarly, AF treatment affected cell cycle progression in BFTC 909 cells. Indeed, the frequency of cells in the S phase increased from 13.61% in the DMSO group to 24.38 and 42.51% after 2 and 4 μM AF treatment for 24 h, respectively (Fig. 3A). However, the increase in the S phase after AF treatment for 48 h was not as evident in BFTC 909 cells (Fig. 3A). Additionally, although there was a small increase in the

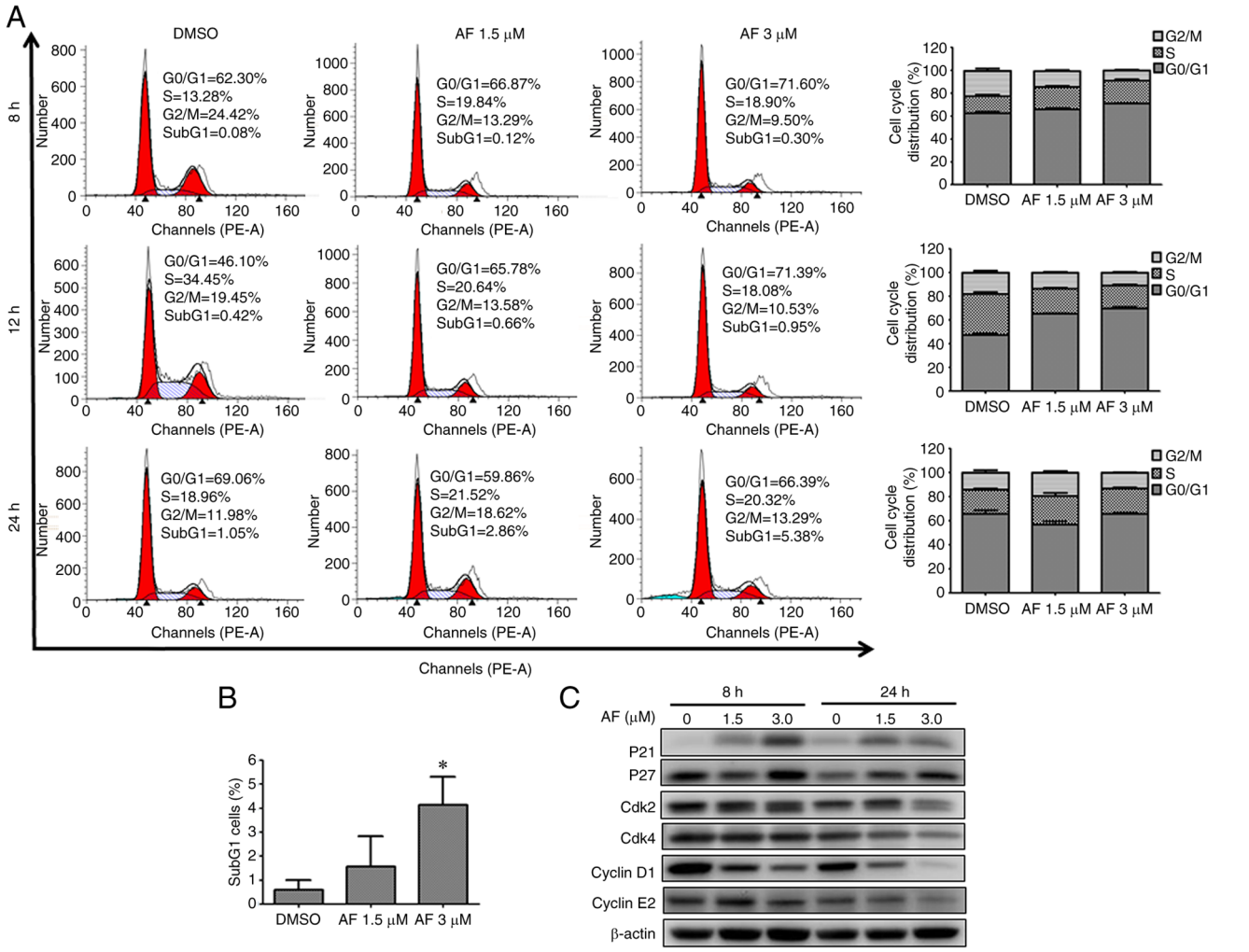

Figure 2. AF induces G0/G1 cell cycle arrest in HT 1376 urothelial carcinoma cells. (A) HT 1376 cells were treated with the indicated concentrations of AF for 8, 12, or 24 h, and cell cycle distribution was analyzed by flow cytometry (left panel). The data from at least three independent experiments are shown and represented as a bar graph (right panel). (B) The frequency of the sub-G1 cell population was determined by flow cytometry. *P<0.05. (C) The expression levels of proteins associated with the cycle were examined in HT 1376 cells treated with the indicated concentration of AF for 8 or 24 h. AF, auranofin.

frequency of subG$_1$ cells, this was not statistically significant (Fig. 3B). CDC25A is thought to play an essential role in G$_1$/S progression (36,37) and the intra-S phase checkpoint by the CDC25A-CDK2 complex (38,39). In addition to an increase of p21 expression, decreased expression of CDC25A and CDK2 was observed in AF-treated BFTC 909 cells (Fig. 3C). The increased expression of p21 and decrease expression of CDC25A suggested that AF treatment caused BFTC 909 cell cycle arrest at the S phase.

Altogether, these findings suggested that AF treatment interfered with cell cycle progression in these UC cell lines, albeit at different phases.

Effects of AF on apoptosis in UC cells. The next experiments were performed to examine whether AF could induce apoptosis in UC cells. The frequency of annexin V$^+$ cells increased in HT 1376 cells after treatment with AF, from 2.4 to 8.7 and 22.8% for the vehicle, 1.5 and 3 μM AF treatment groups, respectively (Fig. 4A, upper panel). However, only the highest concentration (3 μM) of AF treatment produced a statistically significant increase. A small increase in caspase 3 and PARP protein expression was observed after 3 μM AF treatment (Fig. 4A, lower panel), which was consistent with the flow cytometry results. However, AF treatment did not significantly increase apoptosis in BFTC 909 cells (Fig. 4B), with only a slight increase in annexin V$^+$ cells (Fig. 4B, upper panel).

AF exhibits cytotoxicity in UC cells by triggering ROS production. AF has been reported to induce ROS production in several cancer cell types (24-26). Therefore, ROS levels were examined in UC cells after AF treatment in the presence or absence of the ROS scavenger, NAC. AF treatment increased ROS levels in HT 1376 and BFTC 909 cells compared with the vehicle-treated group. However, ROS levels were reduced following co-treatment with AF and NAC compared with AF treatment alone (Fig. 5A). To determine if the cell viability rate would be rescued following a reduction of ROS levels, cell viability was determined in AF-treated HT 1376 and BFTC 909 cells in the presence or absence of NAC. The results showed that cell survival was significantly increased following co-treatment with AF and NAC compared with AF treatment alone, both in HT 1376 (Fig. 5C) and BFTC 909 (Fig. 5D) cells. Thus, these data suggested that AF was cytotoxic to UC cells and interfered with their redox balance.

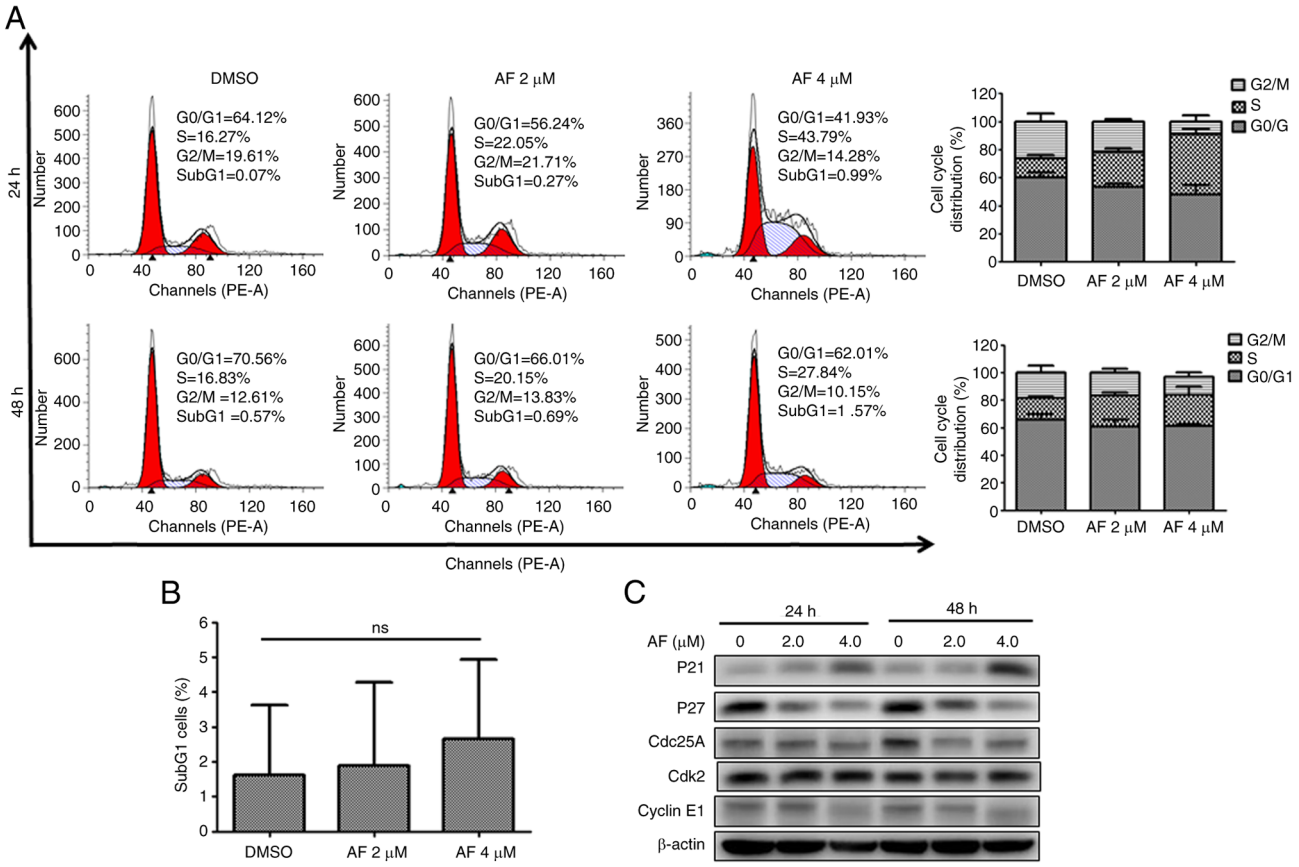

Figure 3. AF induces S-phase cell cycle arrest in BFTC 909 urothelial carcinoma cells. (A) BFTC 909 cells were treated with the indicated concentrations of AF for 8, 12, or 24 h, and cell cycle distribution was analyzed by flow cytometry (left panel). The data from at least three independent experiments are shown and represented as a bar graph (right panel). (B) The frequency of the sub-G1 cell population was determined by flow cytometry. (C) The expression levels of proteins associated with the cycle were examined in BFTC 909 cells treated with the indicated concentration of AF for 8 or 24 h. AF, auranofin.

AF synergizes with cisplatin to inhibit the viability of UC cells. Cisplatin therapy remains the standard chemotherapy for metastatic bladder cancer; however, it is limited by unfavorable toxicity, and only a fraction of patients achieve disease-free survival (9). After determining the cytotoxicity of AF (Fig. 1) and cisplatin in UC cells (Fig. S1), we want to examine the possible synergism of AF and cisplatin in UC cells. Different concentrations of AF and cisplatin were combined to treat UC cells, and cell viability was analyzed using a CCK-8 assay. The CI of AF and cisplatin on HT 1376 cells ranged from 0.232 to 0.302 at 1.5 or 3 μM AF co-treatment with 5 or 10 μM cisplatin and from 0.642 to 0.822 for BFTC 909 cells at 2 or 4 μM AF co-treatment with 15 or 25 μM cisplatin. According to the CI thresholds set by the Calcusyn software, this suggests there was synergism (0.3-0.7) to strong synergism (0.1-0.3) in HT 1376 cells (Fig. 6A). For BFTC cells, there was synergism (0.3-0.7) to moderate (0.7-0.85) (Fig. 6B). Therefore, AF, a drug approved for the treatment of rheumatoid arthritis, may also represent a potential candidate for UC in combination with cisplatin.

Discussion

UC is the most common malignancy in the urinary system. Cisplatin-based combination treatment with surgery remains the standard therapy for patients with MIBC, although its efficacy is limited due to its adverse effects and chemoresistance (9,40). Cancer cells may be more sensitive to ROS-accumulation due to their elevated ROS levels. Increasing ROS generation may have selective cytotoxicity to cancer cells by exhausting the antioxidant system capacity without affecting normal cells (41). In the present study, AF exhibited cytotoxicity towards HT 1376 bladder cancer cells and BFTC 909 upper tract cells by increasing ROS levels. In addition, this compound interfered with cell cycle progression in both cell lines, although cell cycle arrest occurred at different stages. AF induced apoptosis in HT 1376, but not BFTC 909 cells. Furthermore, synergistic cytotoxicity was observed in both HT 1376 and BFTC 909 cells following combined treatment with AF and cisplatin, indicating that this drug may be used for UC treatment.

Drug repurposing (or repositioning) is an attractive approach in the development of new medicines for cancer therapy (42,43). AF, previously used in the treatment of rheumatoid arthritis, has been shown to have anti-proliferation activity in several cancer cell types (44,45). In the present study, the effect of AF in bladder and upper tract UC was examined in HT 1376 and BFTC 909 cells, respectively. The results indicated that AF inhibited the viability of HT 1376 and BFTC 909 cells with a lower IC_{50} in HT 1376 cells, indicating that the HT 1376 cell line is more sensitive to AF treatment. Cancer cells are reported to have elevated ROS levels (12,13), rendering

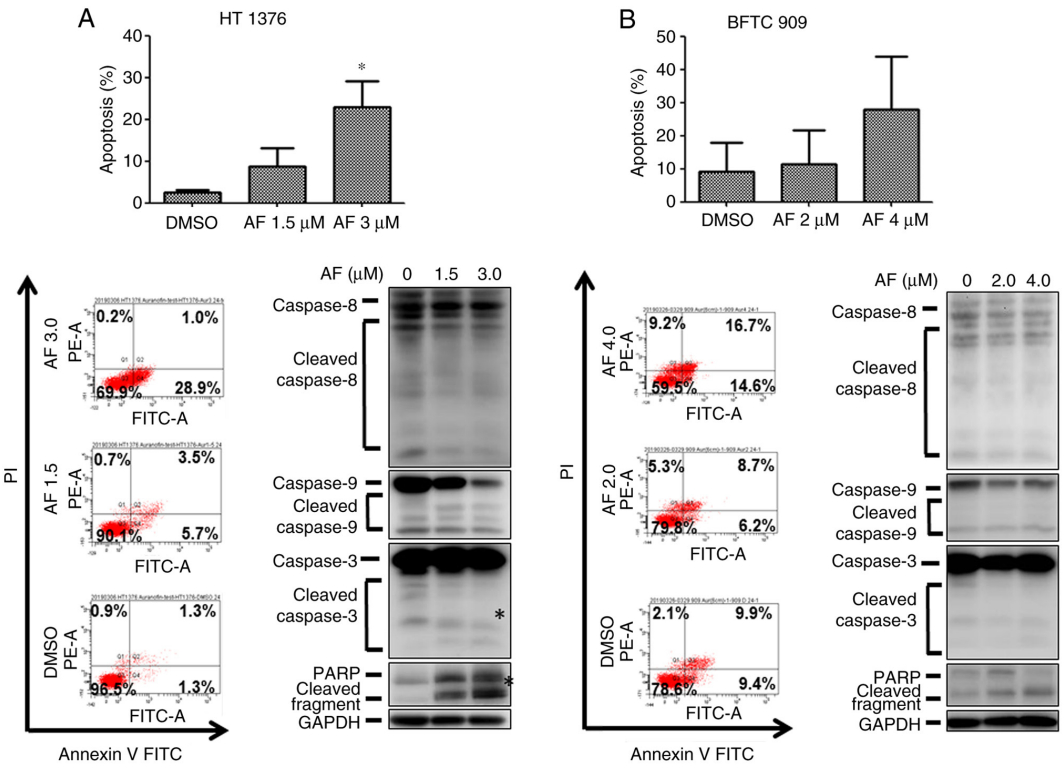

Figure 4. AF induces apoptosis and expression of apoptosis-associated proteins urothelial carcinoma cells. (A) HT 1376 and (B) BFTC 909 cells were treated with the indicated concentrations of AF for 48 h. Apoptotic cells were analyzed by flow cytometry (upper panel). The expression levels of caspase 8, 9 and 3, as well as PARP proteins were analyzed by western blotting (lower panel). *P<0.05. AF, auranofin; FITC, fluorescein isothiocyanate; PI, propidium iodide; PARP, poly (ADP-ribose) polymerase.

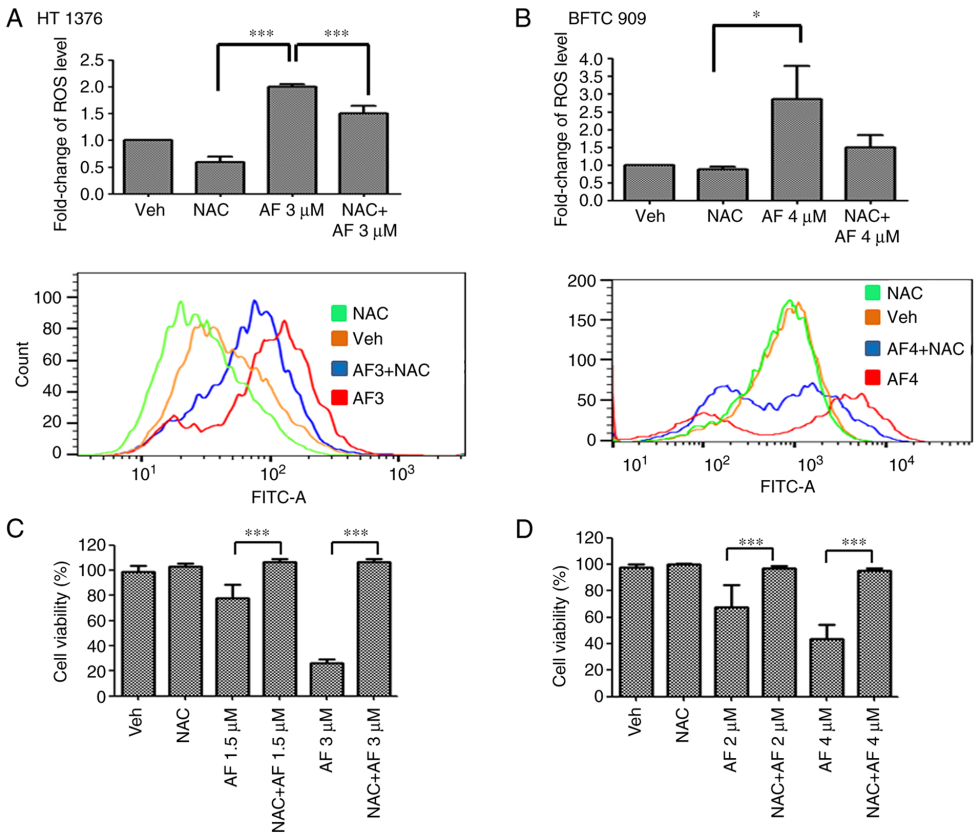

Figure 5. (A) HT 1376 and (B) BFTC 909 cells were treated with the indicated concentrations of AF for 48 h in the presence or absence of NAC. ROS production was determined by flow cytometry (upper panel). Cell viability of (C) HT 1376 and (D) BFTC 909 cells was analyzed using a Cell Counting Kit-8 assay. Data are representative of at least three independent experiments and shown as mean ± SD. *P<0.05; ***P<0.001. AF, auranofin; FITC, fluorescein isothiocyanate; NAC, N-acetyl-L-cysteine; ROS, reactive oxygen species; Veh, vehicle.

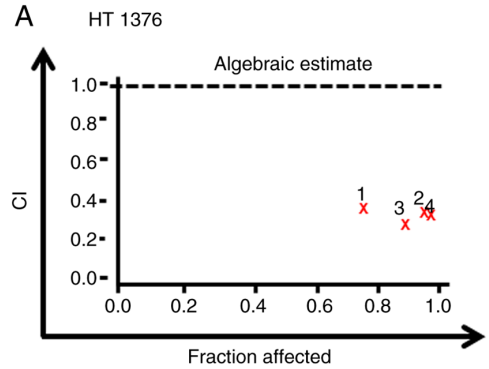

Cisplatin (μM)	Auranofin (μM)	Fraction affect	Combine index
5	1.5	0.76	0.302
5	3	0.94	0.299
10	1.5	0.89	0.232
10	3	0.95	0.293

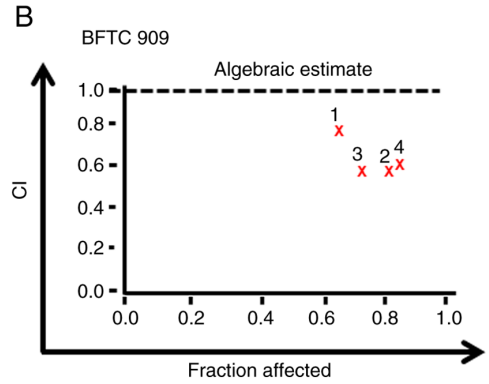

Cisplatin (μM)	Auranofin (μM)	Fraction affect	Combine index
15	2	0.64	0.822
15	4	0.83	0.642
25	2	0.77	0.647
25	4	0.85	0.662

Figure 6. AF synergistically enhances cytotoxicity in cisplatin-treated UC cells. Calcusyn software was used to calculate the CI of AF and cisplatin in UC cells. HT 1376 and BFTC 909 cells were treated with different concentrations of AF and cisplatin, and cell viability was determined using Cell Counting Kit-8 assays. (A) Algebraic estimate represents the combined effect of AF and cisplatin on UC cells. (B) Experimental values for the CI. AF, auranofin; CI, combination index; ROS, reactive oxygen species; UC, urothelial carcinoma.

them more sensitive to ROS induction (15). ROS-producing enzymes are upregulated in UC (27,28). Therefore, drugs that can induce ROS may represent potential candidates for UC treatment. AF increases ROS by targeting thioredoxin reductase (45,46). The reasons underlying the differences observed in the bladder cancer and upper tract urothelial carcinoma cell lines remain unclear. Further analysis of the expression of ROS-reducing enzymes may be needed in order to identify the factors contributing to these difference.

The divergent responses of HT 1376 and BFTC 909 cells to AF treatment were also observed in their cell cycle distribution. HT 1376 were blocked at the G_0/G_1 phase starting at 8 h after AF treatment, whereas BFTC 909 cells showed arrest at S phase 24 h after AF treatment. The expression patterns of cell cycle-associated proteins also supported these results. However, there are limitations in the present study, since we did not check the same panel of cell cycle regulators in both HT 1376 and BFTC 909 cells in our western blotting analysis.

A slight increase in the frequency of $subG_1$ cells was detected after 24-h AF treatment in HT 1376, but not in BFTC 909 cells. Apoptosis was not significantly increased following AF treatment in HT 1376 and BFTC 909 cells. AF treatment has been reported to increase apoptosis in several cancer cell types (44), including lung cancer cells (47) and acute lymphoblastic leukemia (48); thus, our results were inconsistent with these findings, although these results may be due to the different cell lines used. An increase in ROS production can cause DNA damage, which, if continues may signal the cells to cell cycle arrest, ultimately apoptosis will occur (49). Therefore, cell cycle arrest may occur before apoptosis. In the present assay conditions, AF treatment for 24 h did not trigger a significant change in apoptosis rates in BFTC 909 cells, and only higher concentrations of AF had an effect on HT 1376 cells. This suggests a longer AF treatment time may have been necessary for apoptosis to occur in BFTC 909 cells. In addition, a high apoptosis rate was found in DMSO-treated BFTC 909 cells, possibly because the BFTC 909 cells were sensitive to trypsin during the flow cytometric analysis. Thus, the findings on apoptosis need to be treated with caution, as the assay conditions require further optimization.

Another possibility is that a longer AF exposure would be required for the UC cells to exit cell cycle arrest to undergo apoptosis. However, ROS production was increased in both HT 1376 and BFTC 909 cells following AF treatment, and this effect was inhibited in the presence of NAC, a ROS scavenger. In addition, cell viability was increased in the presence of NAC. This suggests that ROS production may cause redox imbalance, which might serve an important role in the effect of AF on the viability of UC cells. Further study is needed to determine the mechanism underlying AF-mediated cytotoxicity in UC cells.

Cisplatin-based chemotherapy remains the standard therapy for patients with advanced UC (8,40,50). Although shifting the regimen of the combination of methotrexate, vinblastine, doxorubicin and cisplatin to gemcitabine + cisplatin demonstrates less toxicity (51,52), cisplatin-based chemotherapy remains relatively toxic. Efforts are needed to develop less toxic, cisplatin-based therapy for patients with advanced UC. Combination therapy of two or more drugs has several benefits, including enhancing efficacy and reducing toxicity (53).

Several molecular mechanisms mediate the antitumor properties of cisplatin (54), such as cisplatin-induced oxidative stress (55). AF treatment synergizes with cisplatin cytotoxicity by ROS production, causing mitochondrial dysfunction and DNA damage in small cell lung cancer (56). The curcuminoid WZ35 inhibits thioredoxin reductase 1 activity, leading to ROS production and thereby enhancing the inhibitory effects of cisplatin on cell viability (57). Therefore, the combination of AF and cisplatin may aggravate redox imbalance, leading to UC cell death.

In summary, AF exhibits anticancer activity in HT 1376 and BFTC 909 cells, interfering with cell cycle progression and redox balance. AF also shows synergism with cisplatin. To the best of our knowledge, these findings are the first to report the effect of AF on the viability of UC cell lines, although further studies are needed to determine the efficacy of AF as potential treatment for UC.

Acknowledgements

Not applicable.

Funding

The present study was supported by The Ditmanson Medical Foundation Chiayi Christian Hospital (grant no. R110-008).

Availability of data and materials

The datasets used and/or analyzed during the current study are available from the corresponding author on reasonable request.

Authors' contributions

SYC designed the research and collected the data. CNC analyzed and interpreted the data. HYH performed the experiments. CYF designed the study and wrote the paper. HYH and CYF confirm the authenticity of all the raw data. All authors have read and approved the final manuscript.

Ethics approval and consent to participate

Not applicable.

Patient consent for publication

Not applicable.

Competing interests

The authors declare that they have no competing interests.

References

1. Yaxley JP: Urinary tract cancers: An overview for general practice. J Family Med Prim Care 5: 533-538, 2016.
2. Sung H, Ferlay J, Siegel RL, Laversanne M, Soerjomataram I, Jemal A and Bray F: Global cancer statistics 2020: GLOBOCAN estimates of incidence and mortality worldwide for 36 cancers in 185 countries. CA Cancer J Clin 71: 209-249, 2021.
3. Lenis AT, Lec PM, Chamie K and Mshs MD: Bladder cancer: A review. JAMA 324: 1980-1991, 2020.
4. Griffiths TR; Action on Bladder Cancer: Current perspectives in bladder cancer management. Int J Clin Pract 67: 435-448, 2013.
5. Ritch CR, Velasquez MC, Kwon D, Becerra MF, Soodana-Prakash N, Atluri VS, Almengo K, Alameddine M, Kineish O, Kava BR, *et al*: Use and validation of the AUA/SUO risk grouping for nonmuscle invasive bladder cancer in a contemporary cohort. J Urol 203: 505-511, 2020.
6. Yafi FA, Aprikian AG, Chin JL, Fradet Y, Izawa J, Estey E, Fairey A, Rendon R, Cagiannos I, Lacombe L, *et al*: Contemporary outcomes of 2287 patients with bladder cancer who were treated with radical cystectomy: A Canadian multicentre experience. BJU Int 108: 539-545, 2011.
7. Perera M, McGrath S, Sengupta S, Crozier J, Bolton D and Lawrentschuk N: Pelvic lymph node dissection during radical cystectomy for muscle-invasive bladder cancer. Nat Rev Urol 15: 686-692, 2018.
8. Patel VG, Oh WK and Galsky MD: Treatment of muscle-invasive and advanced bladder cancer in 2020. CA Cancer J Clin 70: 404-423, 2020.
9. Chamie K, Litwin MS, Bassett JC, Daskivich TJ, Lai J, Hanley JM, Konety BR and Saigal CS; Urologic Diseases in America Project: Recurrence of high-risk bladder cancer: A population-based analysis. Cancer 119: 3219-3227, 2013.
10. Sabharwal SS and Schumacker PT: Mitochondrial ROS in cancer: Initiators, amplifiers or an Achilles' heel? Nat Rev Cancer 14: 709-721, 2014.
11. Pizzino G, Irrera N, Cucinotta M, Pallio G, Mannino F, Arcoraci V, Squadrito F, Altavilla D and Bitto A: Oxidative stress: Harms and benefits for human health. Oxid Med Cell Longev 2017: 8416763, 2017.
12. Cohen Z, Maimon Y, Samuels N and Berger R: Role of reactive oxygen species in the anticancer activity of botanicals: Comparing sensitivity profiles. Oncol Lett 13: 2642-2648, 2017.
13. Kumari S, Badana AK, Mohan GM, Shailender G and Malla R: Reactive oxygen species: A key constituent in cancer survival. Biomark Insights 13: 1177271918755391, 2018.
14. Trachootham D, Alexandre J and Huang P: Targeting cancer cells by ROS-mediated mechanisms: A radical therapeutic approach? Nat Rev Drug Discov 8: 579-591, 2009.
15. Moloney JN and Cotter TG: ROS signalling in the biology of cancer. Semin Cell Dev Biol 80: 50-64, 2018.
16. Chen SY, Huang HY, Lin HP and Fang CY: Piperlongumine induces autophagy in biliary cancer cells via reactive oxygen species-activated Erk signaling pathway. Int J Mol Med 44: 1687-1696, 2019.
17. Lin S, Li Y, Zamyatnin AA Jr, Werner J and Bazhin AV: Reactive oxygen species and colorectal cancer. J Cell Physiol 233: 5119-5132, 2018.
18. Huang H, Xie H, Pan Y, Zheng K, Xia Y and Chen W: Plumbagin triggers ER stress-mediated apoptosis in prostate cancer cells via induction of ROS. Cell Physiol Biochem 45: 267-280, 2018.
19. Zhang L, Li J, Zong L, Chen X, Chen K, Jiang Z, Nan L, Li X, Li W, Shan T, *et al*: Reactive oxygen species and targeted therapy for pancreatic cancer. Oxid Med Cell Longev 2016: 1616781, 2016.
20. Sharma V, Joseph C, Ghosh S, Agarwal A, Mishra MK and Sen E: Kaempferol induces apoptosis in glioblastoma cells through oxidative stress. Mol Cancer Ther 6: 2544-2553, 2007.
21. Zou Z, Chang H, Li H and Wang S: Induction of reactive oxygen species: An emerging approach for cancer therapy. Apoptosis 22: 1321-1335, 2017.
22. Gorrini C, Harris IS and Mak TW: Modulation of oxidative stress as an anticancer strategy. Nat Rev Drug Discov 12: 931-947, 2013.
23. Chaffman M, Brogden RN, Heel RC, Speight TM and Avery GS: Auranofin. A preliminary review of its pharmacological properties and therapeutic use in rheumatoid arthritis. Drugs 27: 378-424, 1984.
24. Lee D, Xu IM, Chiu DK, Leibold J, Tse AP, Bao MH, Yuen VW, Chan CY, Lai RK, Chin DW, *et al*: Induction of oxidative stress through inhibition of thioredoxin reductase 1 is an effective therapeutic approach for hepatocellular carcinoma. Hepatology 69: 1768-1786, 2019.
25. Wen C, Wang H, Wu X, He L, Zhou Q, Wang F, Chen S, Huang L, Chen J, Wang H, *et al*: ROS-mediated inactivation of the PI3K/AKT pathway is involved in the antigastric cancer effects of thioredoxin reductase-1 inhibitor chaetocin. Cell Death Dis 10: 809, 2019.

26. Oh BM, Lee SJ, Cho HJ, Park YS, Kim JT, Yoon SR, Lee SC, Lim JS, Kim BY, Choe YK and Lee HG: Cystatin SN inhibits auranofin-induced cell death by autophagic induction and ROS regulation via glutathione reductase activity in colorectal cancer. Cell Death Dis 8: e3053, 2017.
27. Shimada K, Fujii T, Anai S, Fujimoto K and Konishi N: ROS generation via NOX4 and its utility in the cytological diagnosis of urothelial carcinoma of the urinary bladder. BMC Urol 11: 22, 2011.
28. Miyata Y, Matsuo T, Sagara Y, Ohba K, Ohyama K and Sakai H: A mini-review of reactive oxygen species in urological cancer: Correlation with NADPH oxidases, angiogenesis, and apoptosis. Int J Mol Sci 18: 2214, 2017.
29. Chou TC and Talaly P: A simple generalized equation for the analysis of multiple inhibitions of michaelis-menten kinetic systems. J Biol Chem 252: 6438-6442, 1977.
30. Chou TC and Talalay P: Quantitative analysis of dose-effect relationships: The combined effects of multiple drugs or enzyme inhibitors. Adv Enzyme Regul 22: 27-55, 1984.
31. Chou TC: Theoretical basis, experimental design, and computerized simulation of synergism and antagonism in drug combination studies. Pharmacol Rev 58: 621-681, 2006.
32. Otto T and Sicinski P: Cell cycle proteins as promising targets in cancer therapy. Nat Rev Cancer 17: 93-115, 2017.
33. Malumbres M: Cyclin-dependent kinases. Genome Biol 15: 122, 2014.
34. Sgambato A, Cittadini A, Faraglia B and Weinstein IB: Multiple functions of p27(Kip1) and its alterations in tumor cells: A review. J Cell Physiol 183: 18-27, 2000.
35. Roskoski R Jr: Cyclin-dependent protein serine/threonine kinase inhibitors as anticancer drugs. Pharmacol Res 139: 471-488, 2019.
36. Shen T and Huang S: The role of Cdc25A in the regulation of cell proliferation and apoptosis. Anticancer Agents Med Chem 12: 631-639, 2012.
37. Bartek J and Lukas J: Mammalian G1- and S-phase checkpoints in response to DNA damage. Curr Opin Cell Biol 13: 738-747, 2001.
38. Falck J, Petrini JH, Williams BR, Lukas J and Bartek J: The DNA damage-dependent intra-S phase checkpoint is regulated by parallel pathways. Nat Genet 30: 290-294, 2002.
39. Falck J, Mailand N, Syljuåsen RG, Bartek J and Lukas J: The ATM-Chk2-Cdc25A checkpoint pathway guards against radioresistant DNA synthesis. Nature 410: 842-847, 2001.
40. Drayton RM and Catto JW: Molecular mechanisms of cisplatin resistance in bladder cancer. Expert Rev Anticancer Ther 12: 271-281, 2012.
41. Kim SJ, Kim HS and Seo YR: Understanding of ROS-inducing strategy in anticancer therapy. Oxid Med Cell Longev 2019: 5381692, 2019.
42. Kirtonia A, Gala K, Fernandes SG, Pandya G, Pandey AK, Sethi G, Khattar E and Garg M: Repurposing of drugs: An attractive pharmacological strategy for cancer therapeutics. Semin Cancer Biol 68: 258-278, 2021.
43. Hernandez JJ, Pryszlak M, Smith L, Yanchus C, Kurji N, Shahani VM and Molinski SV: Giving drugs a second chance: Overcoming regulatory and financial hurdles in repurposing approved drugs as cancer therapeutics. Front Oncol 7: 273, 2017.
44. Onodera T, Momose I and Kawada M: Potential anticancer activity of auranofin. Chem Pharm Bull (Tokyo) 67: 186-191, 2019.
45. Zhang X, Selvaraju K, Saei AA, D'Arcy P, Zubarev RA, Arnér ES and Linder S: Repurposing of auranofin: Thioredoxin reductase remains a primary target of the drug. Biochimie 162: 46-54, 2019.
46. Hwang-Bo H, Jeong JW, Han MH, Park C, Hong SH, Kim GY, Moon SK, Cheong J, Kim WJ, Yoo YH and Choi YH: Auranofin, an inhibitor of thioredoxin reductase, induces apoptosis in hepatocellular carcinoma Hep3B cells by generation of reactive oxygen species. Gen Physiol Biophys 36: 117-128, 2017.
47. Cui XY, Park SH and Park WH: Auranofin inhibits the proliferation of lung cancer cells via necrosis and caspase-dependent apoptosis. Oncol Rep 44: 2715-2724, 2020.
48. Karsa M, Kosciolek A, Bongers A, Mariana A, Failes T, Gifford AJ, Kees UR, Cheung LC, Kotecha RS, Arndt GM, *et al*: Exploiting the reactive oxygen species imbalance in high-risk paediatric acute lymphoblastic leukaemia through auranofin. Br J Cancer 125: 55-64, 2021.
49. Kuczler MD, Olseen AM, Pienta KJ and Amend SR: ROS-induced cell cycle arrest as a mechanism of resistance in polyaneuploid cancer cells (PACCs). Prog Biophys Mol Biol 165: 3-7, 2021.
50. Nadal R and Bellmunt J: Management of metastatic bladder cancer. Cancer Treat Rev 76: 10-21, 2019.
51. von der Maase H, Sengelov L, Roberts JT, Ricci S, Dogliotti L, Oliver T, Moore MJ, Zimmermann A and Arning M: Long-term survival results of a randomized trial comparing gemcitabine plus cisplatin, with methotrexate, vinblastine, doxorubicin, plus cisplatin in patients with bladder cancer. J Clin Oncol 23: 4602-4608, 2005.
52. Roberts JT, von der Maase H, Sengeløv L, Conte PF, Dogliotti L, Oliver T, Moore MJ, Zimmermann A and Arning M: Long-term survival results of a randomized trial comparing gemcitabine/cisplatin and methotrexate/vinblastine/doxorubicin/cisplatin in patients with locally advanced and metastatic bladder cancer. Ann Oncol 17 (Suppl 5): v118-v122, 2006.
53. Narayan RS, Molenaar P, Teng J, Cornelissen FMG, Roelofs I, Menezes R, Dik R, Lagerweij T, Broersma Y, Petersen N, *et al*: A cancer drug atlas enables synergistic targeting of independent drug vulnerabilities. Nat Commun 11: 2935, 2020.
54. Dasari S and Tchounwou PB: Cisplatin in cancer therapy: Molecular mechanisms of action. Eur J Pharmacol 740: 364-378, 2014.
55. Saad SY, Najjar TA and Alashari M: Role of non-selective adenosine receptor blockade and phosphodiesterase inhibition in cisplatin-induced nephrogonadal toxicity in rats. Clin Exp Pharmacol Physiol 31: 862-867, 2004.
56. Liu X, Wang W, Yin Y, Li M, Li H, Xiang H, Xu A, Mei X, Hong B and Lin W: A high-throughput drug screen identifies auranofin as a potential sensitizer of cisplatin in small cell lung cancer. Invest New Drugs 37: 1166-1176, 2019.
57. He W, Xia Y, Cao P, Hong L, Zhang T, Shen X, Zheng P, Shen H, Liang G and Zou P: Curcuminoid WZ35 synergize with cisplatin by inducing ROS production and inhibiting TrxR1 activity in gastric cancer cells. J Exp Clin Cancer Res 38: 207, 2019.